



Published in final edited form as:

J Neurosurg. ; 133(3): 839–847. doi:10.3171/2019.6.JNS19541.

First application of 7T ultra-high field diffusion tensor imaging to detect altered microstructure of thalamic-somatosensory anatomy in trigeminal neuralgia

John W. Rutland, B.A.^{1,2}, Kuang-Han Huang, PhD¹, Corey M. Gill, B.S., B.A.², Dillan F. Villavisanis, B.A.³, Judy Alper, M.S.¹, Gaurav Verma, PhD¹, Joshua B. Bederson, M.D.², Bradley N. Delman, M.D., M.S.⁴, Raj K. Shrivastava, M.D.², Priti Balchandani, PhD^{1,4}

¹Translational and Molecular Imaging Institute, Icahn School of Medicine at Mount Sinai, New York, New York, United States

²Department of Neurosurgery, Icahn School of Medicine at Mount Sinai, New York, New York, United States

³Department of Otolaryngology, Icahn School of Medicine at Mount Sinai, New York, New York, United States

⁴Department of Radiology, Icahn School of Medicine at Mount Sinai, New York, New York, United States

Abstract

Object—Trigeminal neuralgia (TN) is a debilitating neurological disease that commonly results from neurovascular compression of the trigeminal nerve (CN V). While CN V has been extensively studied at the site of neurovascular compression, many pathophysiological factors remain obscure. For example thalamic-somatosensory function is thought to be altered in TN, but the abnormalities are inadequately characterized. Further, there are few studies utilizing 7 Tesla MRI to examine TN patients. The purpose of the present study was to use 7 T MRI to assess microstructural alteration in the thalamic-somatosensory tracts of TN patients using ultra-high field MRI.

Methods—10 TN patients and 10 age and sex matched healthy controls were scanned at 7 Tesla MRI with diffusion tensor imaging. Structural images were segmented with an automated algorithm to obtain thalamus and primary somatosensory cortex (S1). Probabilistic tractography was performed between the thalamus and S1 and microstructure of the thalamic-somatosensory tracts was compared between TN patients and controls.

Results—Fractional anisotropy of the thalamic-somatosensory tract ipsilateral to the site of neurovascular compression was reduced in patients (Mean (M) =0.43) compared with side-matched controls (M = 0.47, p = 0.01). Mean diffusivity was increased ipsilaterally in patients

Corresponding Author: John Rutland, Translational and Molecular Imaging Institute, Icahn School of Medicine at Mount Sinai, 1470 Madison Avenue; Floor 1, New York, NY 10129, jack.rutland@icahn.mssm.edu, Tel: 973-255-6562.

Icahn School of Medicine Capital Campaign, Translational and Molecular Imaging Institute and Department of Radiology, Icahn School of Medicine at Mount Sinai

This work has not been previously presented in any manner.

($M = 6.58 \times 10^{-4} \text{ mm}^2/\text{s}$) compared with controls ($M = 6.15 \times 10^{-4} \text{ mm}^2/\text{s}$, $p=0.02$). Radial diffusivity was increased ipsilaterally ($M = 4.91 \times 10^{-4} \text{ mm}^2/\text{s}$) compared with controls ($M = 4.44 \times 10^{-4} \text{ mm}^2/\text{s}$, $p = 0.01$). Topographical analysis revealed FA reduction and diffusivity elevation along the entire anatomical S1 arc in TN patients.

Conclusions—The present study is the first to examine microstructural properties of the thalamic-somatosensory anatomy in TN patients and evaluate quantitative differences compared with healthy controls. The findings of reduced integrity of these white matter fibers provides evidence of microstructural alteration at the level of the thalamus and S1, and furthers our understanding of TN neurobiology.

Keywords

Trigeminal neuralgia; 7 Tesla MRI; diffusion tensor imaging; thalamic-somatosensory tracts; nociception

1. Introduction

Trigeminal neuralgia (TN) is a neurological condition characterized by unilateral pain in the sensory distribution of the trigeminal nerve (CN V). Neurovascular compression of the nerve root entry zone, usually by an artery, is a known cause of TN.^{2,10} Nerve compression has been shown to cause secondary pathology at the conflict site, including demyelination and inflammation, and microvascular decompression is the most effective surgical intervention for this disease.²⁰ Jannetta et al. first proposed “short-circuiting” as the mechanism by which innocuous stimuli trigger painful paroxysms in TN.¹¹ According to this model, demyelination of CN V at the root-entry-zone results in “cross-talk” between low-velocity fibers that carry touch stimuli and pain fibers.¹¹ Therefore, otherwise inoffensive stimuli such as light touch can disproportionately trigger painful paroxysms. This theory aligns with current treatments for TN. Anticonvulsants such as carbamazepine and oxcarbazepine that raise the threshold of excitability are considered the most effective pharmacologic therapies for treatment of TN.¹² Surgical lesioning branches of CN V, thereby reducing afferent input to the affected nerve, is also effective in subduing paroxysmal discharges.¹³ Other treatments aimed at reducing activity of affected nerve fibers, including percutaneous radiofrequency trigeminal gangliolysis, and alcohol or glycerol injection into the trigeminal cistern, have shown varying degrees of success.¹³

More recently, repetitive transcranial magnetic stimulation (rTMS) has been explored as a noninvasive treatment option for patients with TN and other facial pain syndromes.¹⁴ Stimulation is typically applied to the facial region of the primary motor cortex, with the expectation that inhibitory corticocortical feedback will reduce nociceptive activity in the somatosensory cortex.¹⁴ Other neuromodulatory devices currently being vetted for therapeutic roles in the treatment of TN include transcranial direct stimulation¹⁵, direct motor cortex stimulation¹⁶, and deep brain stimulation.¹⁷ While these emerging therapeutics are meant to reduce nociception by lowering excitability in the primary somatosensory cortex, structural substrates of nociception at the level of the thalamus and somatosensory cortex are poorly described in the literature. There is a critical need to ascertain secondary

effects of TN in these regions to further characterize TN pathogenesis and identify novel targets for pain management.

Imaging studies have applied diffusion tensor imaging (DTI) to image CN V and adjacent structures. These studies, which have exploited DTI-based tractography to reconstruct and characterize microstructure of CN V, ^{5,6} commonly report reduced fractional anisotropy (FA) and increased mean diffusivity (MD) at the nerve-root-entry zone. This pattern suggests demyelination of the nerve in proximity to neurovascular conflict.⁵⁻⁸ Recently, a number of studies employing ultra-high field MRI have reported diffusion characteristics of the trigeminal nerve in excellent detail.⁷ Ultra-high field MRI scanners, such as those operating at 7 Tesla (T), offer high spatial resolution and increased signal-to-noise ratio compared with 1.5 and 3T field strengths that are routinely used in the clinical setting. While these studies have characterized structural features of CN V in the region of the nerve root-entry-zone, this technology has not been reported in evaluation of the downstream somatosensory apparatus involved in nociception. Critically, the roles of the thalamus and the somatosensory cortex in mediating pain response in patients with TN remain poorly understood. As new functional therapies that target these regions emerge, microstructural properties of this system should be elucidated in both normal and pathologic states.

The purpose of the present study is to perform high-resolution tractography between the thalamus and primary somatosensory cortex in patients with TN compared to age and sex matched healthy controls, and to evaluate microstructure along these anatomical fibers. This analysis may be useful in characterizing secondary effects of TN pathology and could provide data to support an emerging biomarker that will enhance understanding of TN and pain management in this population.

2. Methods

2.1 Participants

Study approval was obtained from the Institutional Review Board before recruitment. 10 TN patients [6 females, mean age 44.8 years, standard deviation (SD) 17.4 years; 4 males, mean 39.8 years, SD 7.1 years] were recruited through their neurosurgeon (RS) at the Mount Sinai Medical Center between September 2014 and January 2019. Patients were age- and sex-matched with 10 neurologically healthy controls [6 females, mean age 44.2 years, SD 15.2 years; 4 males, mean 40.3 years, SD 6.1 years]. All participants provided written informed consent prior to the study.

2.2. Imaging protocol

Participants were scanned under using a 7T whole body scanner. A SC72CD gradient coil was used along with a single channel transmit and 32-channel receive head coil. The scanning protocol included a high-angular-resolved diffusion-weighted imaging (HARDI) DWI sequence: $b=1200$ mm²/sec, TE=67.6 ms, TR=7200 ms, resolution=1.05 mm isotropic, reversed phase encoding in AP and PA directions for paired acquisition in 64 directions. The DWI post-processing pipeline consisted of skull-stripping, eddy current correction using FMRIB Software Library (www.fmrib.ox.ac.uk/fsl), and correction of gradient

non-linearities. A coronal-oblique T1-weighted MP2RAGE sequence with the following parameters was used for analysis: TE =1.95 ms, TR =3000 ms, flip angle (FA)=7°, field of view (FOV)=320×240-mm², slices=224, resolution=0.7-mm³ isotropic.

2.3 Structural segmentation

MR images were transferred to an in-house workstation for analysis. An automated segmentation software, FreeSurfer image analysis suite version 6.0 (<http://surfer.nmr.mgh.harvard.edu>), was used to segment thalami and postcentral gyri (primary somatosensory cortex [S1]) on T1-weighted MP2RAGE images. ROIs were co-registered to the DTI with Statistical Parametric Mapping 12 in MATLAB (r2017a, The MathWorks). The segmentation methods are shown in Figure 1.

2.4 Tractography

Probabilistic tractography was performed using MRtrix3 with the constrained spherical deconvolution method (Brain Research Institute, Melbourne, Australia). The thalamus and S1 ROIs were used as seedpoints and endpoints, respectively, to reconstruct the thalamic-somatosensory tracts. The default FA threshold of 0.1 and a maximum fiber angle of 60° were selected. Average FA and MD, and axial (AD) and radial (RD) diffusivities were sampled along the thalamic-somatosensory tracts and average metrics were calculated.

To obtain a topographical representation of fiber streamlines, S1 ROIs were converted into spherical coordinates. This simplified S1 into a rough arc, enabling calculation of the relative angle between mid-thalamus and each streamline terminus along the S1 ribbon. All relative streamline angles were then normalized to an angle-index of 0–100, so the most superior streamline has an index of 0 and the most inferior an index of 100. Thalamic-somatosensory tract microstructures were plotted as a function of angle-index.

2.5 Statistical analysis

All statistical analysis was performed using JMP Pro 14.2.0. Wilcoxon two-sided signed rank tests were used to compare microstructural data between matched pairs of TN patients and controls. Microstructure of the thalamic-somatosensory tract on the side of compression was compared to the same side in matched healthy controls. Metrics were also compared between symptomatic and asymptomatic hemispheres within patients. Pearson correlational coefficients were calculated between disease duration, age, and trigeminal distribution and microstructural values. Significance was defined as $p < 0.05$.

3. Results

3.1 Tractography

10 TN patients and 10 age and sex matched healthy controls were scanned at 7T. Demographic information and disease features of TN patients are shown in Table 1. Probabilistic tractography was used to reconstruct the thalamic-somatosensory tracts for all 20 participants, and tractography qualitatively resembled known somatosensory anatomy (Figure 2).

3.2 Thalamic-somatosensory microstructure

Mean FA of the thalamic-somatosensory tracts on the side of neurovascular compression was significantly lower in TN patients ($M = 0.43 \pm 0.04$ [mean \pm SD]) compared with the same side in healthy controls ($M = 0.474 \pm 0.02$, $p = 0.01$). There was no difference between FA values on the side contralateral to compression in TN patients ($M = 0.444 \pm 0.04$) compared with healthy controls ($M = 0.461 \pm 0.02$, $p = 0.6$).

Mean MD of the thalamic-somatosensory tracts on the side of neurovascular compression was greater in TN patients ($M = 6.58 \times 10^{-4} \pm 5.10 \times 10^{-5}$ mm²/s) compared with the same side in healthy controls ($M = 6.15 \times 10^{-4} \pm 1.72 \times 10^{-5}$ mm²/s, $p = 0.02$). MD did not significantly differ between patients in the hemisphere contralateral to compression ($M = 6.44 \times 10^{-4} \pm 3.71 \times 10^{-5}$ mm²/s) and controls ($M = 6.25 \times 10^{-4} \pm 1.31 \times 10^{-5}$ mm²/s) ($p = 0.06$).

There was no difference between mean AD of thalamic-somatosensory tracts in TN patients ($M = 9.93 \times 10^{-4} \pm 6.10 \times 10^{-5}$ mm²/s) compared with the ipsilateral side to the neurovascular compression in healthy controls ($M = 9.56 \times 10^{-4} \pm 2.65 \times 10^{-5}$ mm²/s) ($p = 0.13$). There was also no difference between AD values on the side contralateral to compression in TN patients ($M = 9.84 \times 10^{-4} \pm 5.80 \times 10^{-5}$ mm²/s) compared with healthy controls ($M = 9.64 \times 10^{-4} \pm 1.94 \times 10^{-5}$ mm²/s, $p = 0.6$).

Lastly, mean RD of the thalamic-somatosensory tracts on the side of neurovascular compression was greater in TN patients ($M = 4.91 \times 10^{-4} \pm 5.70 \times 10^{-5}$ mm²/s) compared with the same side in healthy controls ($M = 4.44 \times 10^{-4} \pm 1.88 \times 10^{-5}$ mm²/s, $p = 0.01$). There was no difference between RD values on the side contralateral to compression in TN patients ($M = 4.79 \times 10^{-4} \pm 4.67 \times 10^{-5}$ mm²/s) compared with healthy controls ($M = 4.61 \times 10^{-4} \pm 1.89 \times 10^{-5}$ mm²/s, $p = 0.19$). These results are summarized in Table 2.

There were no significant differences in mean FA, MD, AD, or RD between symptomatic and asymptomatic hemispheres within each patient ($p > 0.05$ for all) (Table 3). Neither duration of disease nor age at time of scan significantly correlate with any of the microstructural properties of the thalamic-somatosensory tracts ($p > 0.05$ for all). Only one patient had V₁ distribution affected and all patients had V₂ distribute affected. The five patients (50%) that had V₃ affected had significantly greater thalamic-somatosensory tract MD and AD in the affected hemisphere than did patients without V₃ involvement, $p < 0.05$ (Table 4).

3.3 Topographical thalamic-somatosensory microstructure

Microstructural properties of the thalamic-cortical tracts on the side of neurovascular compression were spatially normalized and plotted along the arc of S1. FA was consistently lower in TN patients along the entire S1 arc on the symptomatic side. Conversely, MD, AD, and RD were consistently greater in TN patients along the entire trajectory compared with controls (Figure 3).

4. Discussion

Advanced acquisition and post-processing imaging techniques are increasingly being applied to study TN and other complex diseases about the skull base. DTI-based tractography has been used to show diminished CN V integrity at the site of neurovascular compression.^{16,17,19,34} In the present study, ultra-high field MRI enabled advanced DTI-based tractographic reconstruction of the white matter tracts connecting the thalamus and S1. Reduced microstructural integrity of thalamic-somatosensory tracts was found ipsilateral to the site of neurovascular compression in TN patients, while no differences were observed contralateral to the site of neurovascular compression (Figure 4). The tracts on the symptomatic side of each patient were compared to the tracts of the same side for each matched control. These findings may have significant implications for studying TN as well as understanding the fundamental structural substrates mediating nociception and chronic pain.

4.1 Reduced microstructural integrity of thalamic-somatosensory tracts in TN patients

We observed altered microstructural integrity of thalamic-somatosensory tracts in TN patients ipsilateral to neurovascular conflict. These changes include reduced FA and increased MD and RD. FA is a microstructural metric quantifying directionally-constrained water movement, and less-constrained water motion suggested by FA decline is consistent with a demyelinating pathology.²⁴ MD is a sensitive non-directional measure of the magnitude of water diffusion within a voxel that characterizes structural integrity of white matter. Neurological disease is often associated with elevated MD as a result of damaged neuronal membranes.^{24,33} AD and RD are subcomponents of MD that quantify water movement parallel or perpendicular to fibers, respectively.^{14,18,27,28} They likely reflect integrity of axons and myelin, respectively. These metrics are therefore valuable for independently quantifying axon and myelin degradation, two processes by which white matter fibers are affected in neurologic disease with varying underlying neurobiological pathologies.³³ Studies have shown increased AD with axonal damage^{14,18} and elevated RD in demyelinating processes.^{26–28}

The results from the present study suggest that demyelination occurs in fibers connecting the thalamus to S1 in TN patients. Because paroxysms can be triggered by otherwise innocuous sensory stimuli in patients with TN, the role of S1 in TN nociception processing is increasingly being recognized and studied in context of the classic “pain matrix.”^{3,6,31} Blatow et al. employed fMRI to provide evidence of cortical restructuring in patients with TN as a result of CN V hyper-excitation. Their study demonstrated that TN patients showed significantly reduced S1 activation compared with controls.³ Our finding of reduced structural integrity of the thalamic-somatosensory tract, ipsilateral to neurovascular compression may provide an explanation for decreased S1 activation. Interestingly, there were no significant differences in somatosensory-thalamic microstructure between symptomatic and asymptomatic hemispheres within individual patients. Instead, the somatosensory-thalamic tracts in the asymptomatic hemisphere exhibited similar reductions in microstructural integrity as the symptomatic side, however, did not reach statistical significance. As a result, these data could reflect bilateral changes due to the overall level of

pain or the effects of a chronic pain state on the patient. Future studies with larger sample sizes are warranted to determine whether reduction in somatosensory-thalamic tract integrity also exists within the asymptomatic hemisphere.

We also found that patients with V₃ distribution involvement exhibited reduced somatosensory-thalamic tract integrity. Similar statistical analyses could not be performed for V₁ and V₂ distributions because only one patient had V₁ involvement and all patients had V₂ involvement. Our results indicate that V₃ involvement may be associated with reduced somatosensory-thalamic tract microstructure, however, since all patients in this study also had V₂ involvement, it is possible that this finding reflects reduced somatosensory-thalamic tract integrity in patients with more than one affected distribution. Future studies are needed to elucidate the relative contributions of each of the trigeminal distributions in altered somatosensory-thalamic tract integrity in trigeminal neuralgia.

In addition to furthering our understanding of the neurobiology of TN, findings from this study may also have clinical applications, such as with treatment monitoring and predicting response to surgery. For example, prediction of individualized outcomes from decompression surgery in TN remains particularly challenging, and factors contributing to favorable surgical outcomes are inadequately characterized. In their 20-year study of 1185 patients who underwent microvascular decompression for TN, Barker *et al.* reported recurrence and subsequent surgery rates of 30% and 11%, respectively.³ While correlation of imaging with post-operative outcomes was precluded by this study's small sample size, alterations in somatosensory-thalamic connectivity could mediate varying pain responses and may prove useful for prognosis and prediction of ultimate recoverability. Future studies to elucidate the relationship between microstructure of these pathways and postoperative pain remission are warranted and are an area of active investigation in our group.

Results from the present study may also be useful in the context of emerging modulatory neurosurgical treatments for TN. Treatments such as transcranial magnetic modulation and direct motor cortex stimulation aim to lower activity in the primary somatosensory cortex, however, many of these therapies are nascent and are still considered controversial. Multi-modal investigations of thalamic-cortical anatomy may further characterize these circuits and could help identify targets for neuromodulatory intervention in the future.¹⁶ Findings from this study may be relevant for cortical and thalamic targeting for patients with TN, areas of active investigation in our group. These results may also provide useful data that can help predict cross-reactivity with pain medication pathways in patients with TN.

4.2 Topographical representation of thalamic-somatosensory microstructure

In humans, S1 is composed of the well-characterized sensory homunculus, anatomically so that each part of the body maps to a predictable region of the post-central cortex. For example, extremities and trunk of the body are located more superiorly, while the face is positioned more inferiorly. In order to examine integrity of the thalamic-somatosensory tract within regard to different regions of the homunculus innervated, we plotted fiber microstructure in a spatially normalized manner along the arc of S1. The primary purpose of this analysis was to determine whether variation in tract integrity existed within the homunculus, particularly with respect to the facial region. We estimated that the facial

region of the homunculus was between approximately 60°–80° of the S1 arc (Figure 3). Interestingly, this analysis revealed reduced FA and increased MD, AD, and RD along not only the proposed facial region but along the entire S1 arc. These results suggest a global attenuation of thalamic-somatosensory tract integrity as opposed to effect involving only fibers innervating the facial region.

Blatow et al reported reduced functional connectivity of S1 in both the face and finger regions of the somatosensory homunculus, despite the fingers not being implicated in the trigeminal pathway.³ These results, in addition to the topographical findings reported in the present study, suggest that reduced thalamic-somatosensory tract integrity in TN is due to a generalized compensatory deactivation of thalamic-somatosensory processing as opposed to cell injury by trans-synaptic degeneration or neurotoxic electrical insult arising from neurovascular conflict in the region of Meckel's cave.³ Selective degeneration of glutamatergic S1 neurons would provide convincing evidence that generalized reduction in thalamic-somatosensory tract integrity involves a compensatory decoupling of the thalamic-somatosensory system and represents a “top-down” process of pain regulation. This explanation seems especially likely since TN patients who progress to neurosurgery often have a long pain history, giving thalamic-cortical anatomy years to restructure. *Ex vivo* studies aimed at identifying cell types that are susceptible to neuronal loss in S1 are needed to elucidate the mechanism by which the thalamic-somatosensory tracts exhibit compromised microstructure in TN patients.

4.3 Limitations and future directions

The primary limitation of this study was the small sample size. This was partially attributable to contraindications to MRI which are more numerous at ultra-high field and partly because TN is a relatively rare disease with an estimated lifetime prevalence of only 0.3%.³² While a considerable number of TN patients are referred to the author's institution each year, patients eligible for 7T imaging were limited. The limited power may explain why no significant correlations between imaging and disease duration, age, or trigeminal distribution were found in this study. Lack of correlation between imaging and disease duration was unexpected, given that TN is a progressive disease demonstrating gradually worsening symptoms and response to surgery over time. In their review of 252 patients who received neurosurgery for TN, Bederson and Wilson found that symptom duration was associated with postoperative pain remission status, and that patients with symptoms lasting longer than 8 years experienced significantly inferior postoperative outcomes compared with patients with symptom duration of fewer than 8 years.⁴ The average preoperative symptom duration in this study was 3.4 years, and subsequent multicenter studies with larger sample sizes are warranted to determine whether disease duration is associated with structural integrity of thalamic-somatosensory anatomy and elucidate the postoperative outcome correlate of this interaction. Although the degree of pain and sensory loss was not quantitatively examined in this study, correlating thalamic-somatosensory microstructure with extent of nociception is another important area of future investigation. Despite the limited number of participants in this study, significant differences between TN patients and healthy controls were reported, suggesting that 7T DTI acquisition coupled with advanced

post-processing algorithms are sensitive enough to detect subtle microstructural alterations that occur at the level of the thalamus and S1.

The authors performed a topographical analysis of fibers connecting thalamus to S1. The purpose of this examination was to evaluate thalamic-somatosensory tract microstructure in different regions of the homunculus and determine whether spatial variation exists within the somatosensory cortex. While this analysis provided a spatially normalized representation of S1 topography, we acknowledge that the facial homunculus cannot be exactly delineated using our current imaging techniques. Additionally, the undulation and folding of S1 makes precise spatial interrogation of S1 challenging. The topographical analysis reported in this study should be considered a coarse spatial estimate of thalamic-somatosensory microstructure and the approximate location of the facial homunculus is contained in our estimation rather than exactly targeted.

Lastly, we hypothesized that the findings reported in this and previous studies³ reflect a compensatory decoupling of the thalamus and S1 in the chronic pain state, however, other confounding biological mechanisms cannot be discounted at this stage of investigation. For example, trans-synaptic degeneration, an alternative process that could explain our findings of reduced white matter integrity, has been reported in various pathologies including intracranial neoplasms²⁵ and occipital lobe injury¹¹. Similarly, the possibility that the patients in this study exhibited lower thalamic-somatosensory microstructural integrity at baseline, which could predispose them to the TN symptoms, cannot be ruled out given the data presented here. This is an important alternative explanation and future studies comparing these metrics in TN patients to individuals with incidental vascular compression found on routine MRI without TN would provide compelling evidence that the effects of observed in this study are a consequence of vascular compression.

5. Conclusion

This study is the first to employ DTI to reconstruct and quantitatively assess the thalamic-somatosensory tracts in TN patients. The high spatial 7T DTI resolution permitted excellent reconstruction of this anatomy, and produced results that are congruent with known anatomy. The authors leveraged this high-resolution DTI to sample microstructure of the thalamic-somatosensory tracts and identify reduced FA and increased MD and RD of white matter fibers on the side of neurovascular conflict in patients with TN. Interestingly, these alterations were observed along the entire S1 arc, indicating a global decoupling between the thalamus and S1 on the side of neurovascular compression in patients with TN. These changes implicate a compensatory mechanism for reducing pain sensation, and may provide substantial evidence of secondary white matter disruption at the thalamic-somatosensory level in TN patients. The results of this study further the understanding of the neurobiological substrates of TN and remission from chronic pain.

Acknowledgements

Jill Gregory provided medical illustration (Figure 4).

Disclosures

Dr. Priti Balchandani (the Principal Investigator in this study) is a named inventor on patents relating to magnetic resonance imaging (MRI) and RF pulse design. The patents have been licensed to GE Healthcare, Siemens AG, and Philips international. Dr. Balchandani receives royalty payments relating to these patents.

Dr. Balchandani is a named inventor on patents relating to Slice-selective adiabatic magnetization T2-preparation (SAMPa) for efficient T2-weighted imaging at ultrahigh field strengths, Methods for Producing a Semi-Adiabatic Spectral-Spatial Spectroscopic Imaging Sequence and Devices There of, and Semi-Adiabatic Spectral-spatial Spectroscopic Imaging. These patents have been filed through MSIP; they remain unlicensed, there is no discussion to license them in the near future, and there are consequently no royalties revolving around them.

Dr. Joshua Bederson (a Significant Contributor in this study and Chair of the Department of Neurosurgery) owns equity in Surgical Theater, LLC. (manufacturer of the Surgical Navigation Advanced Platform (SNAP) system that may be used for intraoperative image guidance in the study).

The remaining authors report no conflict of interest concerning the materials or methods used in this study or the findings specified in this paper.

Disclosure of funding

NIH R01 CA202911

Abbreviations

AD	axial diffusivity
CN V	trigeminal nerve
DTI	diffusion tensor imaging
FA	fractional anisotropy
MD	mean diffusivity
RD	radial diffusivity
rTMS	repetitive transcranial magnetic stimulation
S1	primary somatosensory cortex
TN	trigeminal neuralgia

References

1. Antal A, Terney D, Kuhn S, Paulus W. Anodal transcranial direct current stimulation of the motor cortex ameliorates chronic pain and reduces short intracortical inhibition. *J Pain Symp Manage* 39:890–903, 2010
2. Apkarian AV, Bushnell MC, Treede RD, Zubieta JK. Human brain mechanisms of pain perception and regulation in health and disease. *Eur J Pain* 9:463–484, 2005 [PubMed: 15979027]
3. Barker FG, Jannetta PJ, Bissonette DJ, Larkins MV, Jho HD, et al. The Long-Term Outcome of Microvascular Decompression for Trigeminal Neuralgia. *N Engl J Med* 334:1077–83, 1996 [PubMed: 8598865]
4. Bederson JB, Wilson CB. Evaluation of microvascular decompression and partial sensory rhizotomy in 252 cases of trigeminal neuralgia. *J Neurosurg* 71:359–67, 1989 [PubMed: 2769387]
5. Blatow M, Nennig E, Sarpaczki E, Reinhardt J, Schlieter M, Herweh C, et al. Altered somatosensory processing in trigeminal neuralgia. *Hum Brain Mapp* 30:3495–3508, 2009 [PubMed: 19365802]

6. Davis KD, Kiss ZH, Tasker RR, Dostrovsky JO. Thalamic stimulation-evoked sensations in chronic pain patients and in nonpain (movement disorder) patients. *J Neurophysiol* 75:1026–1037, 1996 [PubMed: 8867115]
7. Franzini A, Messina G, Cordella R, Marras C, Broggi G. Deep brain stimulation of the posteromedial hypothalamus: Indications, long-term results, and neurophysiological considerations. *Neurosurg Focus* 29:E13, 2010
8. Fromm GH, Terrence CF, Maroon JC. Trigeminal Neuralgia Current Concepts Regarding Etiology and Pathogenesis. *Arch Neurol* 41:1204–7, 1984 [PubMed: 6487105]
9. Hughes MA, Frederickson AM, Branstetter BF, Zhu X, Sekula RF Jr. MRI of the Trigeminal Nerve in Patients With Trigeminal Neuralgia Secondary to Vascular Compression. *AJR Am J Roentgenol* 206:595–600, 2016 [PubMed: 26901017]
10. Jannetta PJ. Arterial Compression of the Trigeminal Nerve at the Pons in Patients with Trigeminal Neuralgia. *J Neurosurg* 26:Suppl:159–62, 1967
11. Jindahra P, Petrie A, Plant GT. The time course of retrograde trans-synaptic degeneration following occipital lobe damage in humans. *Brain* 135:534–41, 2012 [PubMed: 22300877]
12. Kim GM, Xu J, Xu J, Song SK, Yan P, Ku G, et al. Tumor necrosis factor receptor deletion reduces nuclear factor-kappaB activation, cellular inhibitor of apoptosis protein 2 expression, and functional recovery after traumatic spinal cord injury. *J Neurosci* 21:6617–25, 2001 [PubMed: 11517251]
13. Kolodziej MA, Hellwig D, Nimsky C, Benes L. Treatment of central deafferentation and trigeminal neuropathic pain by motor cortex stimulation: Report of a series of 20 patients. *J Neurol Surg A* 77:52–58, 2016
14. Kumar R, Chavez AS, Macey PM, Woo MA, Harper RM. Brain Axial and Radial Diffusivity Changes with Age and Gender in Healthy Adults. *Brain Res.* 2013;1512: 22–36. [PubMed: 23548596]
11. Lie JK, Apfelbaum RI. Treatment of trigeminal neuralgia. *Neurosurg Clin Am* 15:319–334, 2004
15. Love S, Hilton DA, Coakham HB. Central Demyelination of the Vth Nerve Root in Trigeminal Neuralgia Associated with Vascular Compression. *Brain Pathol* 8:1–11, 1998 [PubMed: 9458161]
16. Lutz J, Linn J, Mehrkens JH, Thon N, Stahl R, Seelos K, et al. Trigeminal Neuralgia due to Neurovascular Compression: High-Spatial-Resolution Diffusion-Tensor Imaging Reveals Microstructural Neural Changes. *Radiology* 258:524–30, 2011 [PubMed: 21062923]
17. Lutz J, Thon N, Stahl R, Lummel N, Tonn JC, Linn J, et al. Microstructural alterations in trigeminal neuralgia determined by diffusion tensor imaging are independent of symptom duration, severity, and type of neurovascular conflict. *J Neurosurg* 124:823–30, 2016 [PubMed: 26406792]
18. Metwalli NS1, Benatar M, Nair G, Usher S, Hu X, Carew JD. Utility of axial and radial diffusivity from diffusion tensor MRI as markers of neurodegeneration in amyotrophic lateral sclerosis. *Brain Res* 1348:156–64, 2010 [PubMed: 20513367]
19. Moon HC, You ST, Baek HM, Jeon YJ, Park CA, Cheong JJ, et al. 7.0 Tesla MRI tractography in patients with trigeminal neuralgia. *Magn Reson Imaging* 54:265–270, 2018 [PubMed: 29305127]
20. Mueller D, Obermann M, Yoon MS, Poitz F, Hansen N, Slomke MA, et al. Prevalence of trigeminal neuralgia and persistent idiopathic facial pain: a population-based study. *Cephalgia* 31:1542–8, 2011 [PubMed: 21960648]
21. Nihashi T1, Kakigi R, Okada T, Sadato N, Kashikura K, Kajita Y. Functional Magnetic Resonance Imaging Evidence for a Representation of the Ear in Human Primary Somatosensory Cortex: Comparison with Magnetoencephalography Study. *Neuroimage* 17:1217–26, 2002 [PubMed: 12414262]
22. Obermann M Treatment options in trigeminal neuralgia. *Ther Adv Neurol Diso* 3:107–115, 2010
23. Pollock BE Surgical Management of Medically Refractory Trigeminal Neuralgia. *Curr Neurol Neurosci Rep* 12:125–131, 2011
24. Rovaris M1, Gass A, Bammer R, Hickman SJ, Ciccarelli O, Miller DH, et al. Diffusion MRI in multiple sclerosis. *Neurology* 65:1526–32, 2005 [PubMed: 16301477]
25. Rutland JW, Padormo F, Yim CK, Yao A, Arrighi-Allisan A, Huang KH, et al. Quantitative assessment of secondary white matter injury in the visual pathway by pituitary adenomas: a multimodal study at 7-Tesla MRI. *J Neurosurg* 18:1–10, 2019

26. Sato K, Nariai T, Sasaki S, Yazawa I, Mochida H, Miyakawa N. Intraoperative intrinsic optical imaging of neuronal activity from subdivisions of the human primary somatosensory cortex. *Cereb Cortex* 12:269–80, 2002 [PubMed: 11839601]
27. Song SK, Sun SW, Ramsbottom MJ, Chang C, Russell J, Cross AH. Demyelination revealed through MRI as increased radial (but unchanged axial) diffusion of water. *Neuroimage* 17:14–36, 2002
28. Song SK, Yoshino J, Le TQ, Lin SJ, Sun SW, Cross AH, Armstrong RC. Demyelination increases radial diffusivity in corpus callosum of mouse brain. *Neuroimage* 26:132–40, 2005 [PubMed: 15862213]
29. Tracey I. Nociceptive processing in the human brain. *Curr Opin Neurobiol* 15: 478–487, 2005 [PubMed: 16019203]
30. Tsai YH, Yuan R, Patel D, Chandrasekaran S, Weng HH, Yang JT, et al. Altered structure and functional connection in patients with classical trigeminal neuralgia. *Hum Brain Mapp* 39:609–621, 2018 [PubMed: 29105886]
31. Wang Y, Li D, Bao F, Ma S, Guo C, Jin C, et al. Thalamic metabolic alterations with cognitive dysfunction in idiopathic trigeminal neuralgia: a multivoxel spectroscopy study. *Neuroradiology* 56:685–93, 2014 [PubMed: 24820951]
32. Weber K. Neuromodulation and Devices in Trigeminal Neuralgia. *Headache Currents* 57:1648–1653, 2017
33. Winklewski PJ, Sabisz A, Naumczyk P, Jodzio K, Szurowska E, Szarmach A. Understanding the Physiopathology Behind Axial and Radial Diffusivity Changes—What Do We Know? *Front Neurol* 9:92, 2018 [PubMed: 29535676]
34. Zhang Y, Mao Z, Cui Z, Ling Z, Pan L, Liu X, et al. Diffusion Tensor Imaging of Axonal and Myelin Changes in Classical Trigeminal Neuralgia. *World Neurosurgery* 112:e597–e607, 2018 [PubMed: 29410338]

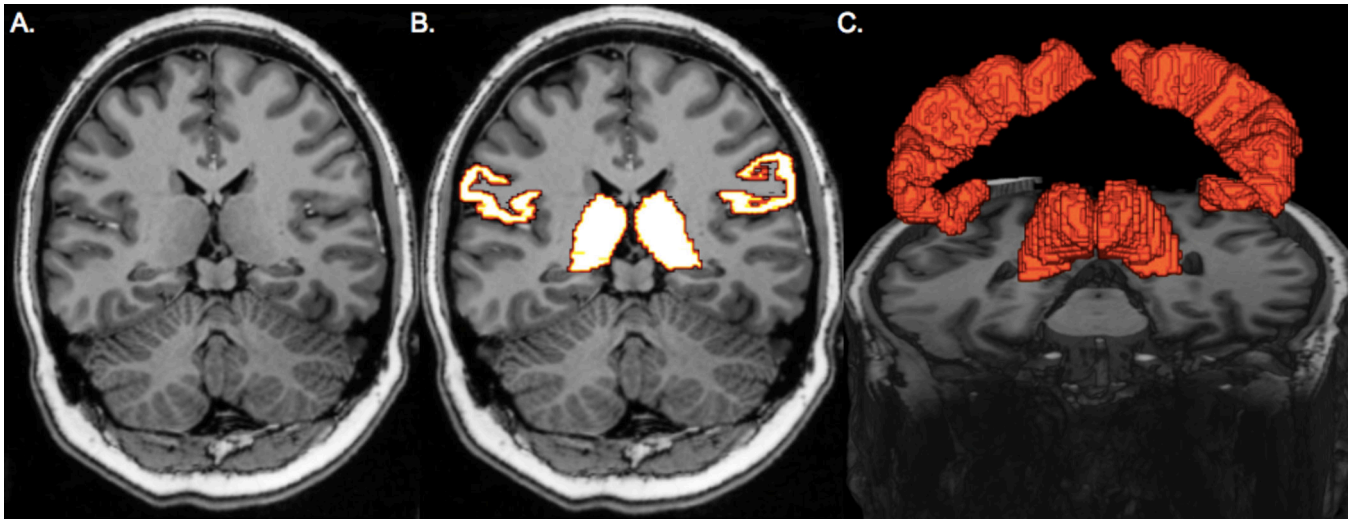


Figure 1. Region of interest selection. Coronal T1-weighted image used for the whole-brain segmentation (A). Thalamic and primary somatosensory cortex segmentation results on coronal T1-weighted image (B). 3-dimensional rendering of thalamic and primary visual cortices (C).

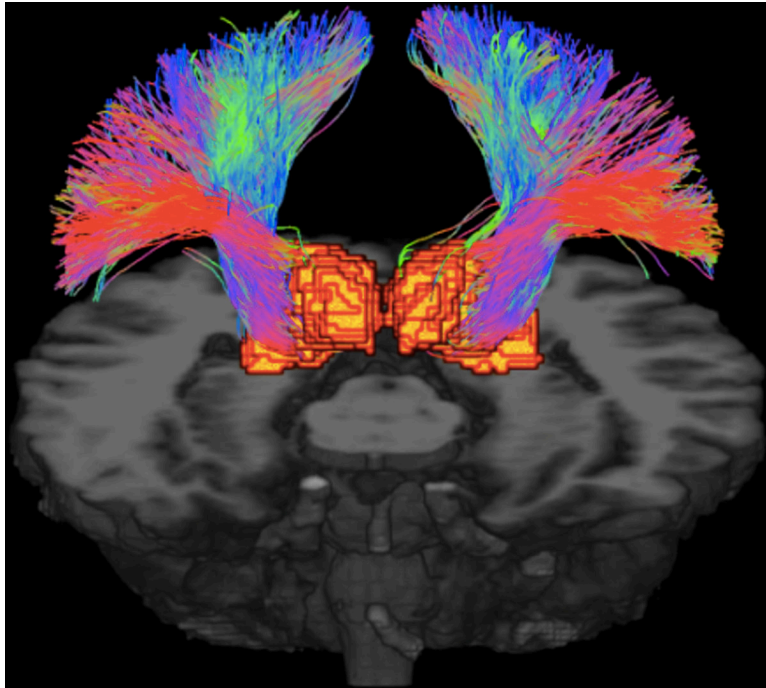


Figure 2. Probabilistic tractography of the thalamic-somatosensory tracts shown in 3-dimensions.

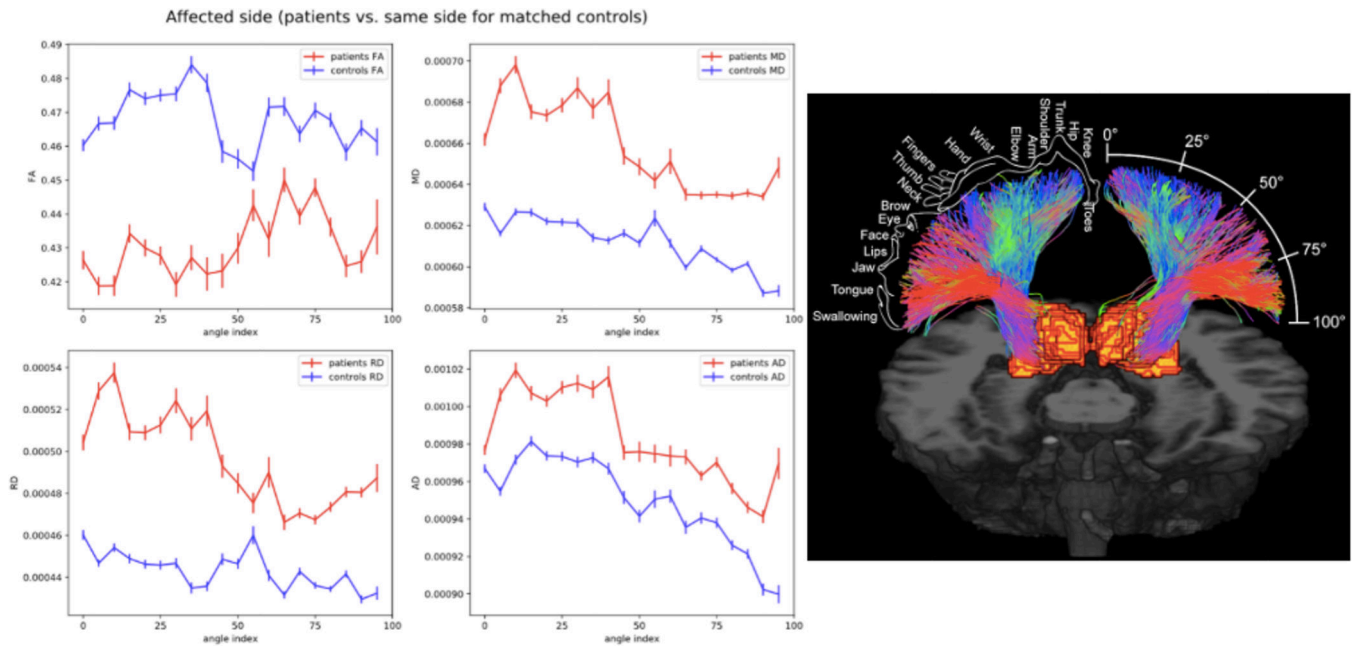


Figure 3. Topographic representation of thalamic-somatosensory tract microstructure on the side of neurovascular compression in TN patients compared with healthy controls (left). Somatosensory homunculus is overlaid on tracts innervating S1 to represent anatomical regions of sensory cortical processing with regard to angle position (right).

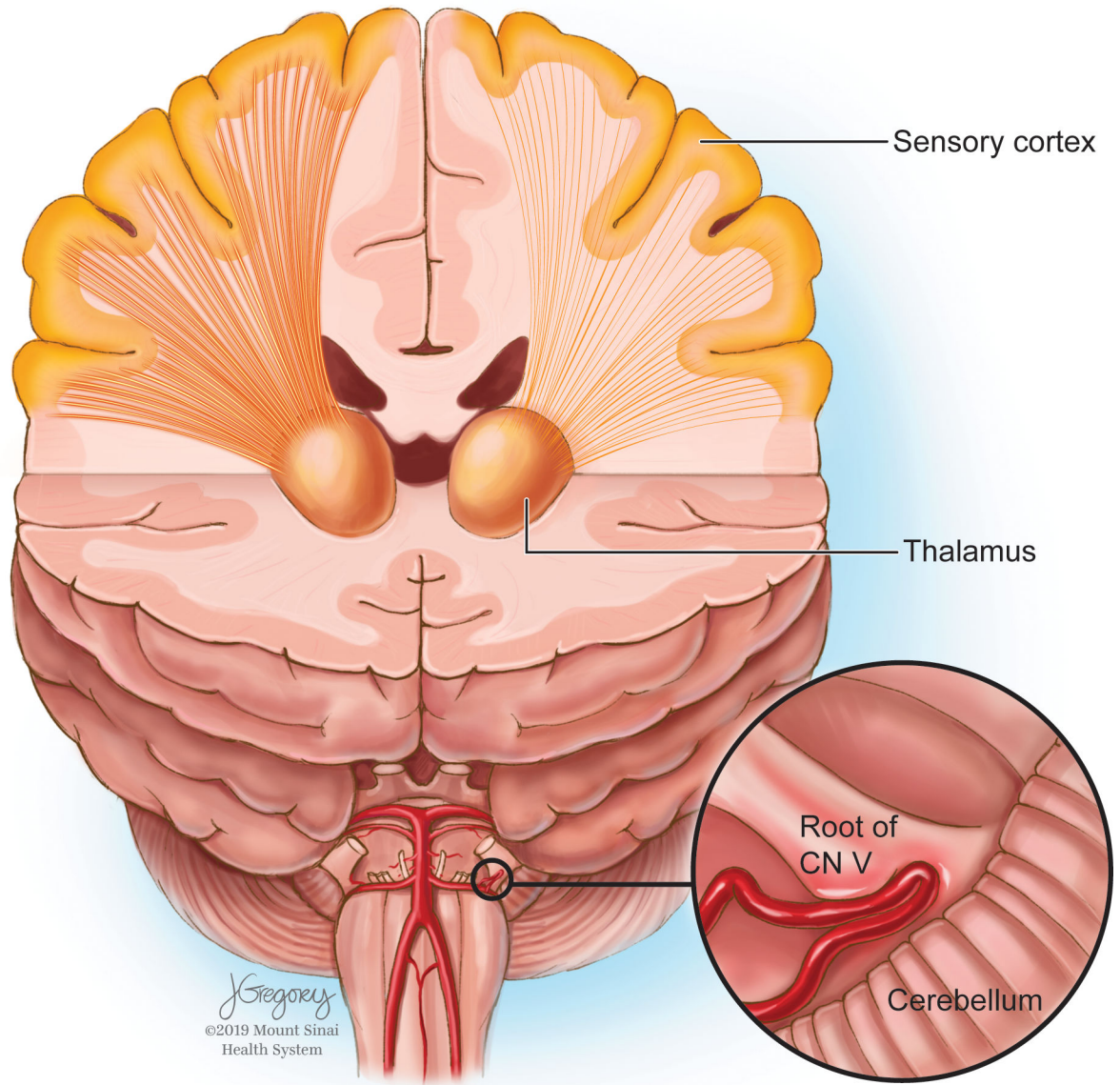


Figure 4. Representation of left-sided neurovascular compression with diminished left thalamic-somatosensory tract integrity.

Table 1.

Demographics and disease features of 10 patients with trigeminal neuralgia

Patient No	Age	Sex	Duration (Months)	Side	Distribution	Imaging features
1	45	M	48	L	V2	Compression of L CN V through a vascular loop
2	66	F	120	R	V2, V3	Vascular compression in proximity of R REZ, 1-mm enhancement in right Meckel's Cave which may represent dilated vessel loop
3	31	M	4	L	V1, V2	Compression lesion via the L REZ
4	48	F	24	L	V2, V3	L posterior fossa epidermoid lesion with extension into prepontine cistern and quadrigeminal plate, clear compression and elevation of CN V at the brainstem origin
5	23	F	1	R	V2, V3	Vascular compression at R CN V root origin
6	38	M	12	R	V2	Ascending artery conflict with R CN V REZ
7	27	F	12	L	V2	L CP angle epidermoid lesion extending from IAC to the back of the clivus and Dorello's canal causing compression of CV V
8	42	M	144	R	V2	Compressive vessel around brainstem interface of the R CN V
9	61	F	36	R	V2, V3	Vascular compression at the R brainstem origin of CN V
10	44	F	12	R	V2, V3	Vascular compression of R trigeminal complex

Table 2.

Thalamic-somatosensory tract microstructural properties in TN patients compared with matched healthy controls. Significance findings are shown in boldface. Diffusivity units expressed in mm^2/s .

	Affected side			Unaffected side		
	Control	TN	p-value	Control	TN	p-value
FA	0.474 (0.02)	0.43 (0.04)	0.01	0.461 (0.02)	0.444 (0.04)	0.60
MD	6.15×10^{-4} (1.72×10^{-5})	6.58×10^{-4} (5.10×10^{-5})	0.02	6.25×10^{-4} (1.31×10^{-5})	6.44×10^{-4} (3.71×10^{-5})	0.06
AD	9.56×10^{-4} (2.65×10^{-5})	9.93×10^{-4} (6.10×10^{-5})	0.13	9.64×10^{-4} (1.94×10^{-5})	9.84×10^{-4} (5.80×10^{-5})	0.60
RD	4.44×10^{-4} (1.88×10^{-5})	4.91×10^{-4} (5.70×10^{-5})	0.01	4.61×10^{-4} (1.89×10^{-5})	4.79×10^{-4} (4.67×10^{-5})	0.19

Author Manuscript

Author Manuscript

Author Manuscript

Author Manuscript

Table 3.

Thalamic-somatosensory tract microstructural properties on symptomatic versus asymptomatic hemispheres within TN patients. Diffusivity units expressed in mm^2/s .

	Symptomatic Hemisphere	Asymptomatic Hemisphere	p-value
FA	0.432 (0.04)	0.446 (0.04)	0.20
MD	6.58×10^{-4} (5.1×10^{-5})	6.44×10^{-4} (3.71×10^{-5})	0.40
AD	9.93×10^{-4} (6.1×10^{-5})	9.84×10^{-4} (5.8×10^{-5})	0.40
RD	4.91×10^{-4} (5.7×10^{-5})	4.78×10^{-4} (4.67×10^{-5})	0.30

Author Manuscript

Author Manuscript

Author Manuscript

Author Manuscript

Table 4.

Comparison of microstructural properties of the thalamic-somatosensory tracts in patients with and without V₃ distribution involvement. Significance findings are shown in boldface. Diffusivity units expressed in mm²/s.

	V3 Affected	V3 Normal	p-value
FA_Affected	0.42	0.44	0.5
FA_Non_Affected	0.45	0.44	0.7
MD_Affected	6.91×10^{-4}	6.257×10^{-4}	0.045
MD_Non_Affected	6.482×10^{-4}	6.401×10^{-4}	0.8
AD_Affected	1.0235×10^{-3}	9.622×10^{-4}	0.037
AD_Non_Affected	9.952×10^{-4}	9.729×10^{-4}	0.6
RD_Affected	5.248×10^{-4}	4.574×10^{-4}	0.06
RD_Non_Affected	4.897×10^{-4}	4.676×10^{-4}	0.5

Author Manuscript

Author Manuscript

Author Manuscript

Author Manuscript